Conventional versus ComputerAssisted Techniques for Reconstruction of Orbitozygomatic Fractures

Thesis

Submitted for Partial Fulfilment of the Requirements for the Doctor's Degree in Oral and Maxillofacial Surgery

Ву

Yasmine Ahmed Nassar B.D.S, M.Sc.

Faculty of oral and Dental Medicine,
Cairo University

2012

Supervisors

Dr. Maha Mohamed Hakam

B.Ch.D., M.Sc., Ph.D. (Cairo)

Professor of Oral and Maxillofacial Surgery, Faculty of Oral and Dental Medicine - Cairo University.

Dr. Ahmed Abd ElMonoem Barakat

B.Ch.D., M.Sc., Ph.D. (Cairo)

Professor of Oral and Maxillofacial Surgery, Faculty of Oral and Dental Medicine - Cairo University.

Dr. Khaled Mahmoud Abd ElGhany

Associate Professor, Head of Rapid Prototyping Dept.

Central Metallurgical Research and Development Institute, Ministry of Scientific Research and Technology.

Acknowl edgement

My deepest thanks and gratitude goes to Dr. *Maha Hakam*; my dearest professor. You have been really supportive, generous and responsible. Without your guidance this work would have never been accomplished.

My deepest sense of gratitude goes to Dr. *Ahmed Barakat*, your highly motivated character added positively to this research.

I would also like to thank Dr. *Khaled Abd ElGhany* for his generosity and support that paved the way for this work.

No words can express what I owe to my husband, colleague and friend *Adel Abou-ElFetouh* whom I consider an integral part of this research for all what he has done. I am really indebted.

Words cannot also express how grateful I am to Dr. *Amr Maher*, who has been always enlighting and generous.

Last but not least, I would like to thank my colleagues in the department of Oral and Maxillofacial surgery. Special thanks go to *Mohamed Faramawy*, *Amira Moussa*, *Mahmoud Hanafy*, *Mohamed Moneer*, *Youssef Akoush*, *Tarek Faramay*, *Salma Hassan* and *Ahmed Youssef* for their help.

DeDication

This piece of work is dedicated to
my parents and grandmother (who bless my life).

A special dedication to my husband; Adel Abou-ElFetouh,
my son Omar, my daughter; Yasmine
and my sisters; Maha and Hanan.

Table of ConTenTs

	Page
List of Abbreviations	ii
List of Figures	iv
List of Tables	vii
Introduction	1
Surgical Anatomy	3
Review of Literature	10
Aim of Study	37
Patients and Methods	38
Results	66
Discussion	80
Summary and Conclusions	87
References	90
Arabic Summary	103

LIST OF ABBREVIATIONS

2D	Two dimensional
3D	Three dimensional
ALT	Alanine Transaminase
ANOVA	Analysis of variance
AST	Aspartate Transaminase
CAD/CAM	Computer Aided Design/ Computer Aided Manufacture
CD	Compact Disc
CNC	Computer Numerical Control
CT	Computed Tomography
DICOM	Digital Imaging and Communication In Medicine
gr.	Group
HDPE	High Density Porous Polyethylene.
I.M.	Intramuscular
INR	International Normalized Ratio
LASER	Light Amplification by Stimulated Emission of Radiation
MRI	Magnetic Resonance Imaging
MVA	Motor Vehicle Accident
no.	Number

NOE	Naso-Orbito-Ethmoidal
PDS	Poly Dioxanone.
PT	Prothrombin Time
PTT	Partial Thromboplatin Time
SPSS	Statistical Package for Social Sciences
Std.	Standard
STL	Steriolithographic
UV	Ultra Violet

LIST OF FIGURES

Figure	Description	Page
1	Different bones contributing to the bony orbit.	3
2	Jackson's classification of orbitozygomatic fractures.	10
3	A diagram illustrating the upward sloping of the floor posteriorly in intact orbits.	15
4	Two dimensional (2D) cuts of a CT scan of a right unilateral orbitozygomatic complex fracture, direct axial cut with a displaced lateral orbital wall fracture (a), reconstructed coronal cut showing a fracture within the body of the zygomatic bone (b) and a reconstructed sagittal cut showing orbital floor fracture (c).	43
5	A reconstructed coronal view of the bony structures before (a), and after (b) bone thresholding.	45
6	3D image of bone showing the multiple fractures and displacement of the right orbitozygomatic complex and zygomatic arch, frontal view (a), lateral view (b).	45
7	Segmentation of the soft-tissue and air (pink), in the 2D images.	46
8	The maxillary sinus and part of the ethmoid air sinus highlighted (red).	46
9	The created 3D image of the air sinuses (red) within the skull (translucent yellow).	47
10	The mirroring process of the intact bony side (yellow and red) onto the fractured side (beige and green).	47
11	Seperation fractured segments of the zygomatic bone (blue and pink) was performed.	48
12	Virtual reduction of the fractured segments of the zygomatic bone (red and pink) on the 3D image.	49
13	Facial symmetry checked by mirroring the intact zygoma	49

	onto the virtually repositioned zygoma.	
14	The final form of the fractured side (the right side) after merging the virtual images of the reduced bony segments and the mirrored air sinuses.	50
15		51
15	The virtual image of a template designed to hold the reduced upper segment (red) to the intact superior orbital rim above.	31
16	A three dimensional image for the part of the orbit to be converted into a resin model (a), and for a zygomatic template (b).	51
17	The individually designed stereolithographic orbital model with the titanium mesh bent on the model.	52
18	The postseptal transconjunctival approach with lateral canthotomy	54
19	Carroll- Girard bone-screw screwed into the body of the left zygoma.	55
20	Top view of the right zygomatic bone exposed through a bicoronal approach.	56
21	The final position of the right zygomatic bone after fixation.	57
22	The titanium mesh placed to cover the entire orbital defect and fixated anteriorly using microscrews. At the inferior orbital rim a miniplate can be also seen after fixation.	58
23	Seperation of the orbital contents from the surrounding structures in the coronal (a), axial (b) and the sagittal (c) cuts.	61
24	3D image for the orbital contents and the eyelids after separation (a). The cutting plane (green) designed to define the anterior boundary of the bony orbit (b).	62
25	The cutting plane passing within the orbital rim and separating the orbital contents from the soft-tissue situated outside the boundaries of the bony orbit (a). A 3D image of the orbital contents (b).	63
26	An axial cut of a CT scan, with a line measuring the	64

	distance between the maximum convexity of the globe and	
	the midpoint of the superior orbital fissure (left orbit).	
27	Pre- and postoperative photographs of patient no. 4 in	65
	group 1. A right orbitozygomatic complex fracture.	
28	Pre- (a) and postoperative (b) photographs of patient no. 5	65
	in group 1.	
29	Pre- (a) and postoperative (b) photographs of patient no. 3	66
	in group 2.	
30	Pre- (a) and postoperative (b) photographs of patient no. 4	66
	in group 2.	
31	Preoperative CT scan of patient no. 5 in group 1.	67
32	Postoperative CT scan patient no. 5 in group 1.	67
33	Preoparative CT scan axial cut of patient no. 3 in group 2.	68
34	Postoparative CT scan axial cut of patient no. 3 in group2.	68
35	A bar chart of the mean orbital volumes of intact,	70
	traumatized and reconstructed orbits of group1.	
		5 0
36	A bar chart showing the mean orbital volumes of intact,	72
2=	traumatized and reconstructed orbits of group2.	5 0
37	A bar chart demonstrating the difference in orbital volumes	73
20	among group 1 and group 2.	77.4
38	A bar chart comparing the accuracy of orbital volume	74
20	reconstruction in groups 1 and 2.	75
39	A bar chart of the mean pre- and postoperative values for	75
40	the degree of enophthalmous in group 1.	7.6
40	A bar chart of the mean pre- and postoperative values for	76
4.1	the degree of enophthalmous in group 2.	77
41	A bar chart of the pre- and posteoperative degrees of	77
	enophthalmous in both groups.	

LIST OF TABLES

Table	Description	Page
1	Group1 patients' preoperative clinical data.	39
2	Group 2 patients' preoperative clinical data.	40
3	The age range in the studied groups.	40
4	The time lapse between trauma and surgery in the studied groups.	41
5	Volumetric measurements of group1.	70
6	Volumetric measurements in group 2	72
7	Comparison of the orbital volumes of both groups.	73
8	Comparison of the accuracy of both reconstructive techniques.	74
9	The pre- and postoperative degrees of enophthalmous in group1.	75
10	The pre- and postoperative degrees of enophthalmous in group2.	76
11	Comparison of the pre- and postoperative degrees of enophthalmous of both groups.	77

Orbitozygomatic injuries need a multidisciplinary approach. Cases should be planned individually to reconstruct orbital structures, restore the cosmetic appearance and visual functions. Bony structures should be repositioned in their original place in space, soft tissues re-suspended where they used to be before the injury and scars should be revised. Complex posttraumatic orbital deformities might need multiple operations to correct, starting with a bony reconstruction⁽¹⁾.

Inaccuracy in reconstructing the orbitozygomatic complex may lead to impairment of function, such as diplopia, or unacceptable esthetics, such as cases of hypoglobus or enophthalmous. Achievement of this goal is sometimes very challenging due to the anatomical nature of this area.

The routine practice in planning such traumatic cases is mainly dependant on clinical and radiographic findings, including those presented as three dimensional (3D) radiographic data in computerized tomography (CT) scans.

Although the CT scans with the ability of reconstruction into three dimensional images are useful in giving an insight to the details of bony fractures, but alone they might not be enough for the transfer of the surgical plan accurately to the operating room. So, not until the development of surgical planning software accompanied with the ability of producing physical models has the transfer of a preoperative plan been possible, a practice that expanded in the past 2 decades⁽²⁾. The costs of such techniques may limit their use as a routine practice, except if they prove to be cost worthy, in terms of accuracy and significant improvement in the clinical outcome. Therefore a comparison of the conventional "free-hand" technique

Introduction

and "computer-assisted" techniques was deemed necessary to test the feasibility of the computer-assisted techniques in reconstruction of orbitozygomatic fractures.

The bony orbit resembles a quadrilateral pyramid which becomes three sided near its apex, with an average volume of 30 cm³⁽³⁾. At the orbital rim the average horizontal dimension is 40 mm while the vertical dimension is about 35 mm, but the orbit is at its widest dimension 1cm behind the orbital rim⁽⁴⁾. The base of the orbit is anterior with a slight lateral and downward angulations while its apex orbit is shifted medially. The orbit is formed of seven bones, namely the maxillary, lacrimal, ethmoidal, sphenoidal, zygomatic, frontal and palatine bones^(5,6) (*figure 1*).

The orbital rim acts as a thick gate to the thin roof, floor, medial and lateral walls of the orbital cavity, and this is of special significance in dissipating forces away⁽⁷⁾. The middle thirds of the orbital walls are thin and therefore are more prone to fracture⁽⁸⁾.

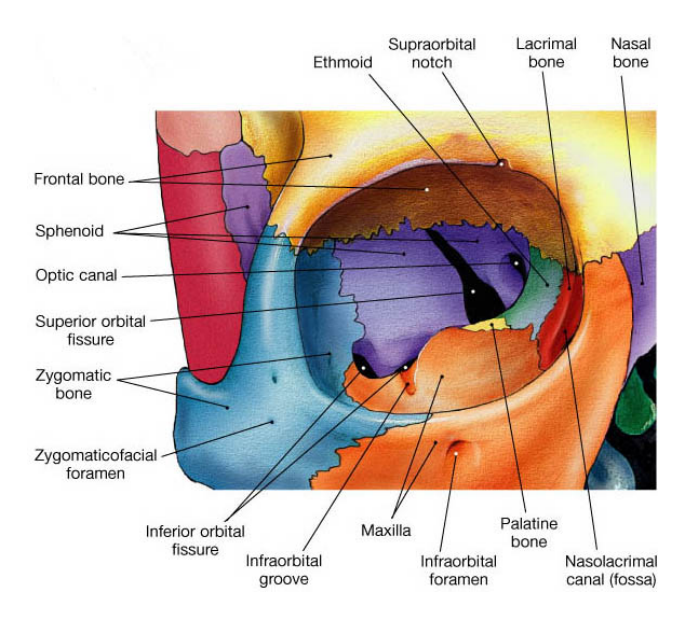


Figure 1: Different bones contributing to the bony orbit⁽⁹⁾.

The orbital floor

The floor of the orbit slopes upwards posteriorly and is formed by the orbital process of the maxilla, the orbital process of the zygoma and posteriorly by part of the palatine bone⁽⁵⁾. It is often 0.5 mm thin. The lateral border of the floor is made by the inferior orbital fissure which separates the floor from the lateral wall posteriorly⁽¹⁰⁾. A safe subperiosteal dissection is considered 20 - 25 mm from the inferior orbital rim⁽⁶⁾.

The infraorbital groove emerges from the middle of the inferior orbital fissure to run anteriorly. It originates 2.5 - 3 cm posterior to the inferior orbital rim, and transfers into a canal midway between the orbital rim and the inferior orbital fissure. Medial to the infraorbital groove, at the junction of the medial wall and the floor, the orbital floor is very thin due to the expansion of the maxillary sinus in this region⁽⁴⁾. Since the equator of the globe lies at or just behind the lateral orbital rim one can appreciate the value of the posterior region of the orbit and its contents in maintaining the anterior position of the globe⁽¹¹⁾.

The medial wall

The medial wall is formed, from anterior backwards, by the frontal process of the maxilla, the lacrimal bone, the ethmoid bone and the lesser wing of the sphenoid. The medial walls are parallel and about 2.5 cm apart. The thinnest part is the lamina papyracea (0.2 - 0.4 mm)⁽¹²⁾, which is that part of the ethmoid air sinus covering the ethmoid air cells lying medially^(4, 5). A study was performed to analyze areas of the medial wall which are most prone to fracture, it was found that the anterior part of the lamina